J MATER SCI 41 (2006) 3349–3355

Compression of homogeneous and graded SiC/EP rings: experimental results and FE modelling

P. TSOTRA, K. FRIEDRICH
Institut für Verbundwerkstoffe GmbH, University of Kaiserslautern, Erwin-Schrödinger-Strasse, 67663, Kaiserslautern, Germany

D. FELHOS, K. VARADI*
Institute of Machine Design, Technical University Budapest, Müegyetem rkp. 3, 1111, Budapest, Hungary
E-mail: varadik@eik.bme.hu

Published online: 12 April 2006

Functionally graded rings based on an epoxy matrix and SiC fillers were prepared and subjected to a compression test. For comparison, rings with homogeneous filler concentration and neat epoxy were also tested. The homogeneous and the graded rings showed the tendency to break at different locations. In order to have accurate information about the material properties, tension and compression tests were performed on isotropic specimens having various SiC volume fractions. The FE simulations of the compressed rings verified the experimental data, as the stress/strain components in the representing locations were able to predict the failure. © *2006 Springer Science + Business Media, Inc.*

1. Introduction

Functionally graded (FG) materials constitute a new class of materials in which the composition and/or the microstructure varies in one specific direction, resulting in corresponding changes in the properties of the material [1–3]. Those gradients in the material properties are engineered, meaning intentionally altered, and quantitatively controlled in order to achieve improvement in mechanical or other properties of the final component.

The FG research area has been spreading into many fields of applications such as mechanical, electrical, nuclear, and optical [3]. Furthermore, the FG concept is actively extended from ceramic/metal materials, where it was initially introduced, to organic composite materials. Carbon fibres have been incorporated in epoxy resin targeting to the creation of a gradient in electrical conductivity [4–6]. Moreover, epoxy resins with SiC particles have been used for creating FG materials with controlled hardness and wear resistance over the cross section of the samples [7, 8]. One very promising field of application for the FG structures is related to the cylinders used by the papermaking industry. In this case, structures with enhanced mechanical and wear properties on their outer layer are requested.

The aim of the present work was to study the behaviour of graded SiC/epoxy rings under compression loads with the use of FE modelling. For comparison rings with homogeneous filler concentration and neat epoxy matrix were also tested and modelled. Different fracture behaviour was detected between the homogeneous and graded rings, which was verified by the FE analysis.

2. Experimental results

The thermosetting matrix used in this study was an epoxy resin (EP), cured with an amine hardener. SiC particles were used as filler material. The particles had an irregular angular shape.

In order to obtain a good dispersion of the SiC particles in the EP matrix the mixing took place in a dissolver device (Dispermat AE, VMA-Getzmann GmbH). For the preparation of the graded rings, mixtures of 5 vol.% SiC were poured into cylindrical moulds. The graded SiC distribution was created by centrifuging the mould at 1000 rpm for 30 min. Rollers with isotropic SiC content (5 vol.%) and neat EP were also prepared. From the cured rollers, rings were obtained by cutting perpendicular to the centrifugation axis. The rings had the inner/outer diameter of 50/65 mm with longitudinal thickness of 9 mm.

The compression test of the rings was carried out using a universal testing machine (Zwick 1485, Germany). Three specimens of each type of rings were tested with a

*Author to whom all correspondence should be addressed.
0022-2461 © *2006 Springer Science + Business Media, Inc.*
DOI: 10.1007/s10853-005-5388-8

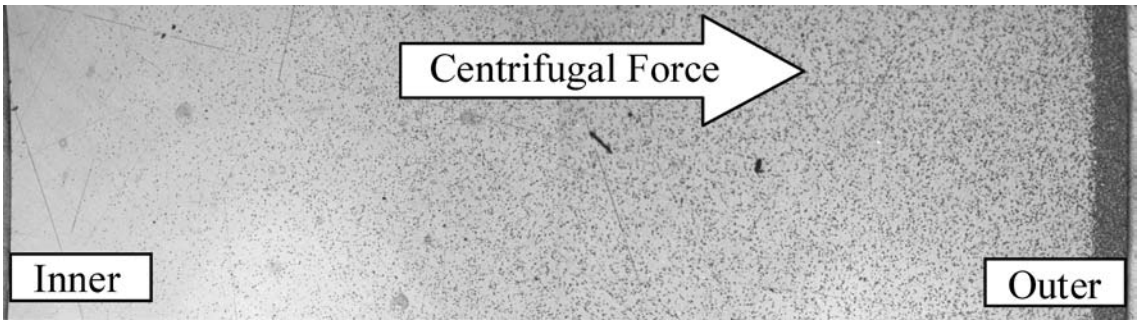

Figure 1 Light optical micrograph showing the SiC distribution of the FG ring (Ring thickness in radial direction: 7.5 mm).

cross-head speed of 1 mm/min. The local microhardness at every 0.25–0.5 mm along the radial direction of the FG rings was determined on polished samples cut parallel to this direction. The measurements were performed with a Vickers indenter, with a load range of 1500 mN and a loading-unloading speed of 70 mN/s.

2.1. Determination of the local filler fraction in radial direction

The SiC distribution along the radial axis of the FG ring is illustrated in Fig. 1, as it was observed by light optical microscopy. The first step for modelling the stresses and strains in FG rings was to determine the SiC distribution along the radial direction. Due to the small radial thickness of the developed FG ring an indirect way was followed. The graded microhardness profile along the radial direction was initially defined (Fig. 2). Lower microhardness (*HU*) values were observed near the inner region of the ring while *HU* reached very high values at the outer region of the ring. Moreover, the microhardness of homogeneous specimens with various SiC contents was also measured. In this way, a "master-curve" showing the *HU* as function of the SiC volume fraction was obtained (Fig. 3). The *HU* values for SiC contents above 30 vol.% were extrapolated, as no specimens could be prepared for such concentrations due to the high viscosity of the mixtures.

The local *HU* value was used in order to define the corresponding SiC volume fraction of the FG rings according to Fig. 3. Similar technique has been used also by

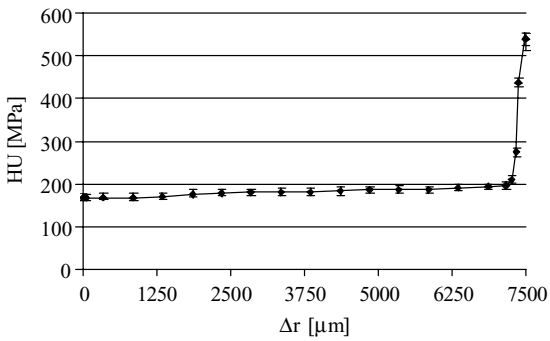

Figure 2 Universal hardness (*HU*) profile along the radial direction (Δr) of the FG ring.

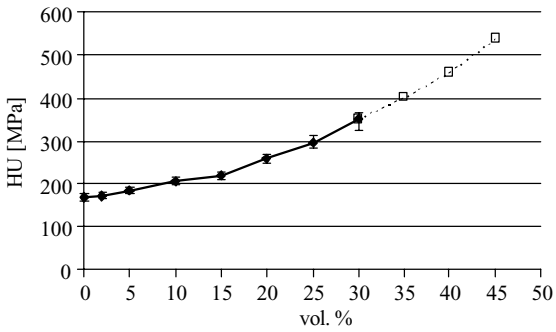

Figure 3 Universal hardness (*HU*) of specimens containing different SiC volume content (the dotted line corresponds to the extrapolated values).

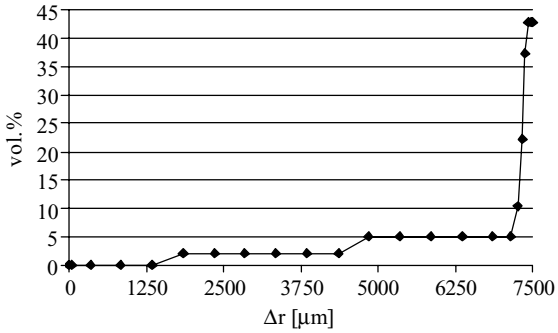

Figure 4 SiC volume content distribution along along the radial direction (Δr) of the FG ring.

Watanabe *et al*. [2] for obtaining information on the composition gradients of alumina fibres in ceramic matrix. The profile of the graded SiC distribution along the radial axis of the FG ring is presented in Fig. 4. Very high concentrations (>40 vol.%) are observed at the outer region of the graded ring. As it was mentioned previously, isotropic samples with so high SiC concentrations were not possible to be prepared by simple mixing process. However, the centrifugation technique gives the possibility to develop composites with highly filled regions due to the forced movement of the fillers under the centrifugal force.

2.2. Mechanical properties of isotropic SiC/EP composites

During the compression test the rings are subjected to tensile and compression stresses. In order to have

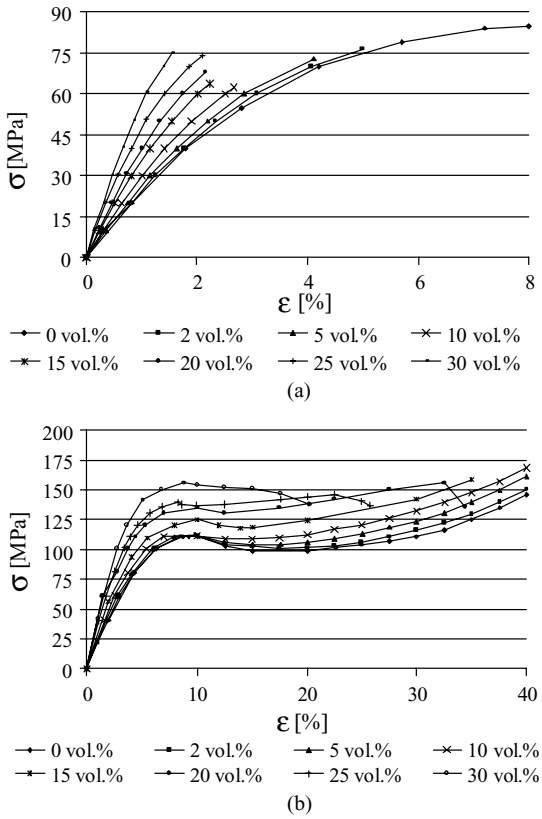

Figure 5 (a) Tensile and (b) compressive σ-ε curves of the various SiC/EP composites.

accurate information about the material properties, tension and compression tests were performed on isotropic specimens having various SiC volume fractions (5, 10, 15, 20, 25 and 30%). The stress-strain curves for tension and compression are presented in Figs 5a and b, respectively. In the case of compression tests, the real stress-strain curve was determined, as the cross-section of the specimen changes considerably during the loading.

Both the neat resin (EP) and the SiC/EP composites bear greater deformation under compression than under tension.

2.3. Ring compression tests

In Fig. 6 the force-displacement curves during the compression loading of the three types of rings are presented. The EP ring bears greater deformation than the rings containing SiC particles; the former shows a more plastic behaviour. The rings containing SiC particles—the homogeneous ring and FG ring—bear less deformation; however, they are stiffer than the EP ring.

During the compression tests it was detected that the breakage of the EP and homogeneous rings with SiC particles initiated from the inner surface of the ring, always at the upper or lower location (Fig. 7a). In the case of the FG rings failure took place in different location. It initiated from the outer surface of the rings, at the left or right side of the horizontal plane of symmetry (Fig. 7b).

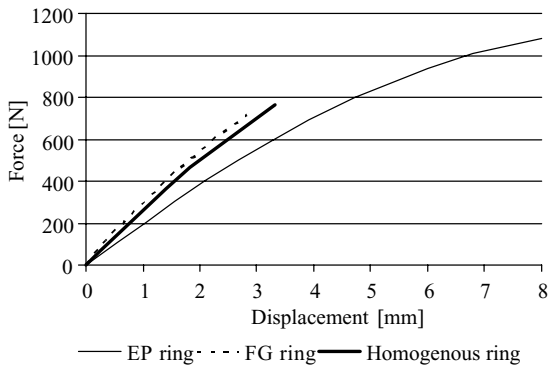

Figure 6 Force-displacement curves during the compression of the various rings.

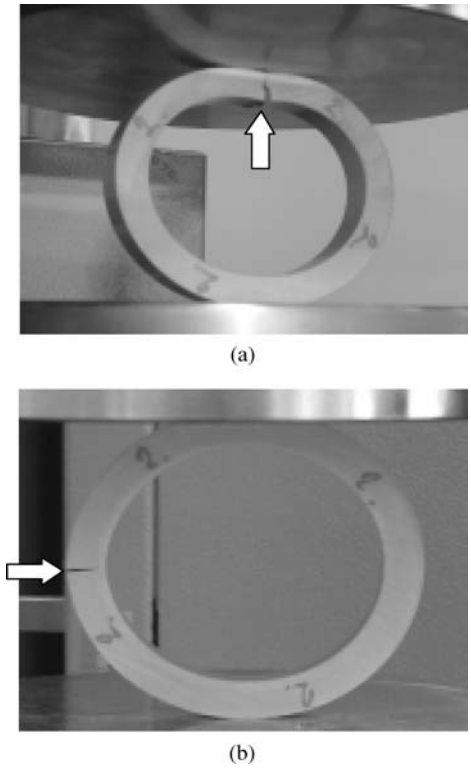

Figure 7 Failure of rings under compression: (a) homogeneous ring, and (b) FG ring. Arrows indicate the direction of failure initiation.

In Fig. 8 the fracture surfaces of the homogeneous and the FG rings are compared, taken from the failure locations, shown in Fig. 7. The homogeneous ring (Fig. 8a) shows a rough fracture surface which corresponds to a higher deformation observed in Fig. 5a (strain-to-failure is about 4%). On the other hand, for the FG ring a finer fracture surface is observed. In this case, the failure initiates from the outer region of the ring, which is highly filled with SiC particles (>40 vol.%). According to Fig. 5a, small deformations are expected for composites containing such a large amount of reinforcing particles.

In Fig. 9 the distribution of the tensile and compression zones in deformed rings is illustrated for homogenous case. According to this figure the different failure behaviour of the rings can be explained. The fracture

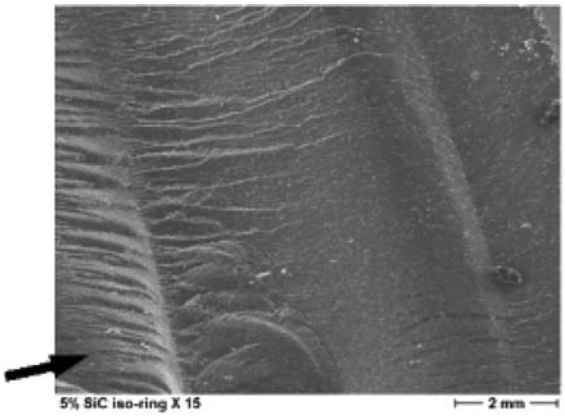

(a)

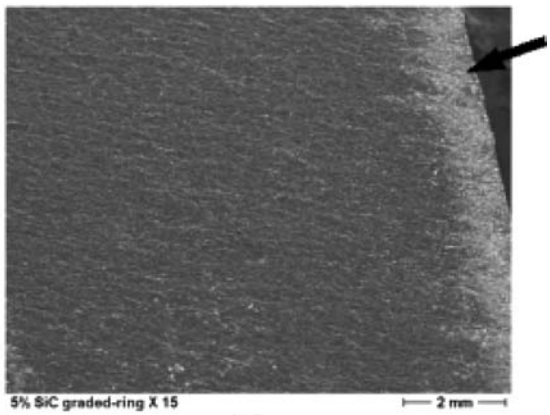

(b)

Figure 8 Fracture surfaces of a) homogeneous and b) FG ring. The arrows indicate the direction of failure initiation.

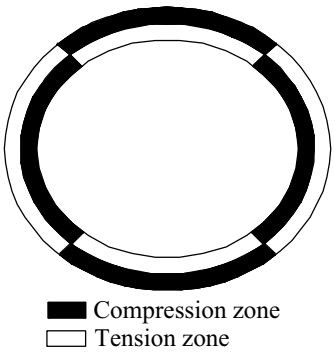

Figure 9 Estimated distribution of the various load zones in the deformed ring for homogenous case.

location of the EP and homogeneous ring is within a tension zone. Such behaviour was expected as these rings bear much greater compression than tensile load (Fig. 5). In the case of FG rings, the failure phenomenon occurs in the horizontal plane, along the outer surface, which is also within a tensile zone. Failure does not take place in the upper tensile zone, because in this zone contains hardly any reinforcing material (see Fig. 1). According to Fig. 5a, the higher is the SiC concentration in EP matrix, the easier is to break under tensile loading. Along the outer surface of the FG rings, where breakage occurs, SiC particles are accumulated in a considerably high volume content.

3. FE modelling

The FE models used in this study are built up of PLANE2D elements of COSMOS/M system, assuming plane strain. Fig. 10a shows the structure of the mechanical model of the ring and the compressive plate. Taking advantage of the two axis of symmetry, a quarter model was used. The material characteristics of steel were assigned to the pressure plate; the contact between the specimen and the pressure plate was established by the use of contact elements. A non-linear material model was utilized. The related FE model in Fig. 10b, shows an enlarged part of the model indicating the various layers of the FG ring. The corresponding stress-strain (σ-ε) curves for each layer were assigned. The compressive σ-ε curves were associated with the compression zones while the tensile σ-ε curves with the tension zones assumed.

The FE calculations were non-linear; including both material and geometric non-linearity. Solutions were force-control-driven, applying the modified Newton-Rapson method. The models contain 19402 nodes, 19029 elements, and 60 contact elements.

3.1. EP ring

Fig. 11 shows the FE results corresponding to the EP ring. The stress-strain results at the locations A, B, C and D are summarised in Table I. The FE results were in good agreement with the failure processes observed during the compression loading of the rings. As it was mentioned previously the breakage of EP rings occurs always in the upper tensile zone. Neat EP exhibits tensile and compression strength of approx. 87 MPa and 200 MPa, respectively. The same material reaches maximum strain of about 8% under tensile and 40% under compression loading. According to Table I the largest tensile stress and strain are generated at location B. Although at location A a greater compression stress is generated, failure will occur at the point of maximum tensile stress as the matrix material can bear lower stress and deformation under tensile loads.

TABLE I Stress and strain values at characteristic locations in the case of EP ring. The B and C columns corresponds to tensile zones, while the A and D columns to compression zones

	A	B	C	D
σ_x (MPa)	−130	97.8	0.04	0.44
σ_y (MPa)	−30.8	0.13	67.1	−93.4
σ_z (MPa)	−41.9	42.9	23.8	−22.5
σ_{Mises} (MPa)	94.7	84.8	58.9	84.8
ε_x (%)	−6.63	7.53	−1.7	1.51
ε_y (%)	0.67	−5.27	3.16	−4.93
ε_z (%)	0	0	0	0
ε_{eq} (%)	4.66	7.42	2.85	3.89

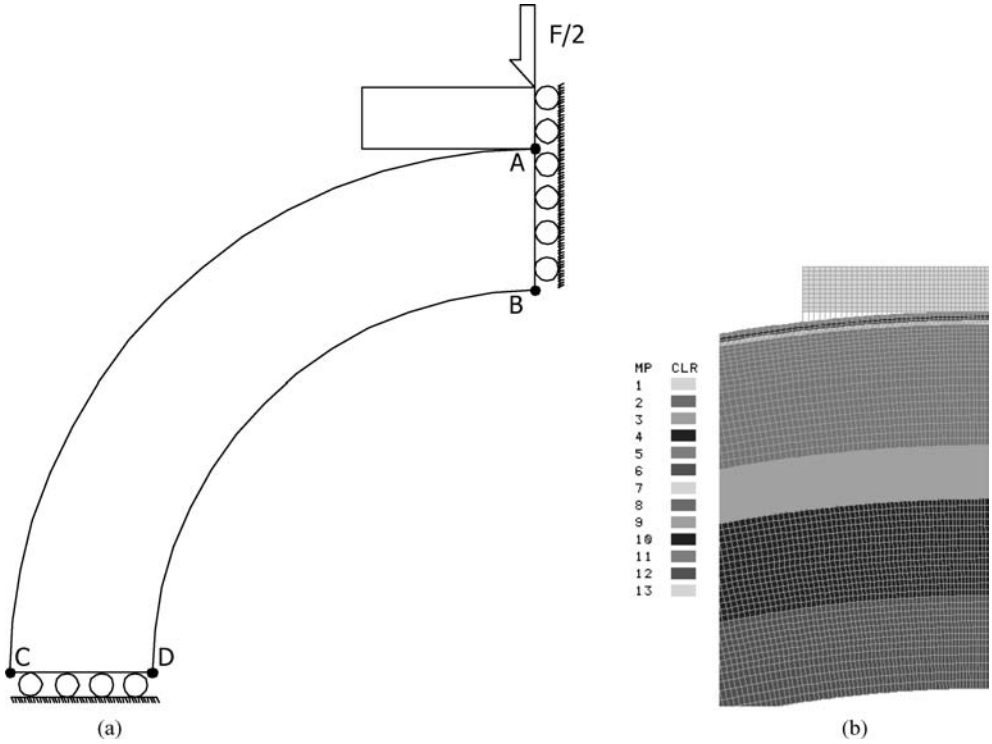

Figure 10 (a) The structure of the mechanical model of the ring and the compressive plate (b) Layers of the FE model of the FG ring.

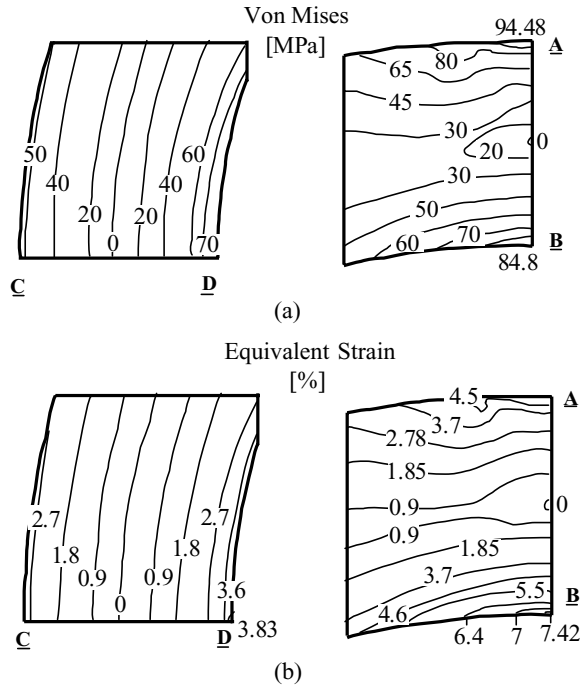

Figure 11 (a) Stress distribution σ_{Mises} and (b) Equivalent strain ε_{eq} of the EP ring at the failure load (1085 N).

3.2. SiC filled homogeneous ring

In Table II the FE results for the homogeneous ring are presented. The same tendency as in the case of EP ring is observed: the largest tensile stress and deformation occur in the upper tensile zone at location B, and therefore the ring fails at this position. The composite containing 5 vol.% SiC has a strength value of approx. 175 MPa under compression and 72 MPa and tension loading, approximately. Moreover, it exhibits 40% equivalent strain under compression and 4% under tension loading. In this case, the compression stresses do not approach the value of compression strength at any location of the ring, neither the degree of failure strain under compression load is reached. However, the value of tensile strength and failure deformation are approached at the location B. This means that the homogenously filled ring will break at the upper or lower tensile zone.

3.3. FG ring

In case of the FG ring, breakage occurred at the left or right side of the ring in the horizontal plane, within the tensile zone. The reason for this is that the matrix contains

TABLE II Stress and strain values at characteristic locations in the case of homogenously filled ring. The B and C columns corresponds to tensile zones, while the A and D columns to compression zones

	A	B	C	D
σ_x (MPa)	−95.7	78.8	−0.02	−0.14
σ_y (MPa)	−36.4	0.25	42.2	−57.2
σ_z (MPa)	−29.2	29.9	13.8	−12.1
σ_{Mises} (MPa)	63.2	68.7	37.2	52.1
ε_x (%)	−3.81	3.63	−0.73	0.65
ε_y (%)	−0.43	−2.1	−1.52	−2.49
ε_z (%)	0	0	0	0
ε_{eq} (%)	2.41	3.34	1.33	1.91

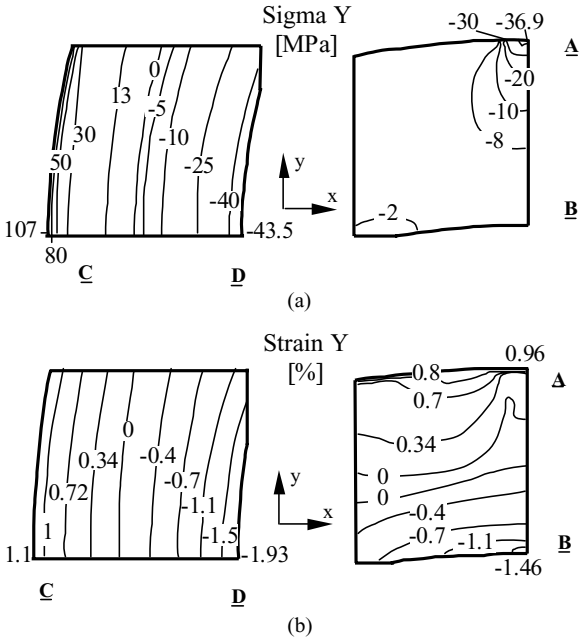

Figure 12 (a) Stress distribution σ_y and (b) Strain ε_y in *y*-direction of the FG ring at failure load (713 N).

hardly any reinforcing particles in the upper tensile zone, and therefore its tensile strength is higher than that is the left or right tensile zone.

Figs. 12a and b show that high tensile stresses in the *y*-direction are generated in the surface layer of the ring. This is due to the high SiC concentration of this layer. At high SiC volume contents, the elastic modulus of the material is quite high, and therefore high tensile stresses are generated. According to Table III, the location A shows maximum compression stress. However, the degree of strain (2.6%) is not so high in order to result in failure of the ring. Considering the tensile stresses, location C is the critical point. Really high tensile stress of approx. 107 MPa is generated here, together with a critical degree of strain (about 1.1%). This may represent failure of the composite with 42.8 vol.% SiC under tensile loads. Thus, in the case of the FG ring, the failure location observed experimentally corresponds to the critical location found by the FE calculations.

TABLE III Stress and strain values at characteristic locations in the case of the FG ring. The B and C columns corresponds to tensile zones, while the A and D columns to compression zones

	A	B	C	D
σ_x (MPa)	−188	−5.07	−0.006	−0.01
σ_y (MPa)	−36.9	−6.13	107	−43.5
σ_z (MPa)	−79.3	−3.36	42.8	−13.1
σ_{Mises} (MPa)	135	10.2	93.6	38.5
ε_x (%)	−2.6	2.81	−0.67	0.82
ε_y (%)	0.96	−1.46	1.1	−1.93
ε_z (%)	0	0	0	0
ε_{eq} (%)	2.12	2.51	1.01	1.63

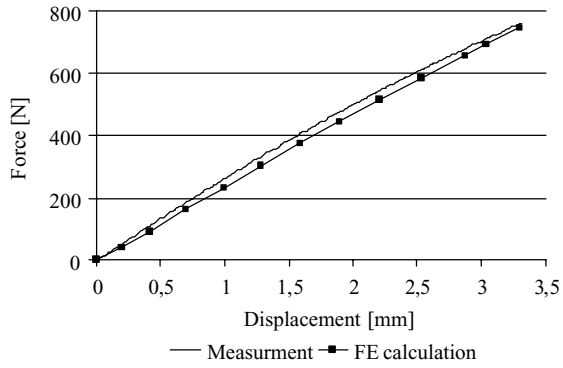

Figure 13 Force vs. displacement curves for compression tests of FG rings.

Fig. 13 shows that the experimental and FE force-displacement curves are in good agreement. The FE models of the rings with various material structures can therefore simulate the real behaviour of the rings.

4. Conclusions

Based on the experimental results and FE calculations of the neat EP, the SiC/EP homogeneous and graded composites the following conclusions can be derived:

- The 2D quarter model with a layered structure approximates properly the behaviour of ring specimens under compression loading, if the material characteristics are associated to the corresponding stress—strain curves both for the tensile and compression zones are considered.
- The behaviour of neat resin and the SiC/EP composites is different under tensile and compression loading. They exhibited much larger strength under compression than under tension.
- The graded SiC distribution along the cross-section of the FG ring can be indirectly evaluated by a set of microhardness measurements, as well as using a set of specimens with homogeneous SiC distributions.
- Rings of homogeneous and graded distribution break at different locations during compression loading. In the case of rings with homogeneous distribution, breakage occurs in the upper or lower tensile zone whereas in the case of graded distribution at the tensile zones in the horizontal plane.

Acknowledgments

The authors gratefully acknowledge the support of BMBF-TÉT as part of the German-Hungarian research cooperation.

References

1. T. HIRAI, in "Materials Science and Technology: a Comprehensive Treatment" (Weinheim, VCH Verlagsgesellschaft GmbH, 1996) 295.
2. Y. WATANABE and Y. FUKUI, *Aluminium Transactions*. **2** (2000) 195.
3. W. A. KAYSSER and B. ILESCHNER, *MRS Bulletin* (1995) 22.

4. N. J. LEE, J. JANG, M. PARK and C. R. CHOE, *J. Mat. Sci.* **32** (1997) 2013.
5. *Idem. Compos. Part.* **A34** (2003) 75.
6. P. TSOTRA and K. FRIEDRICH, *Compos. Sci. Techn.* **64** (2004) 2385.
7. M. KRUMOVA, C. KLINGSHIRN, F. HAUPERT and K. FRIEDRICH, *ibid.* **61** (2001) 557.
8. C. KLINGSHIRN, M. KOIZUMI, F. HAUPERT, H. GIERTZSCH and K. FRIEDRICH, *J. Mater. Sci. Let.* **19** (2000) 263.

Received XXX
and accepted 14 July 2005